

Transient absorption of vibrationally excited water

H. J. Bakker and H.-K. Nienhuys

FOM Institute for Atomic and Molecular Physics, Kruislaan 407, 1098 SJ Amsterdam, The Netherlands

G. Gallot, N. Lascoux, and G. M. Gale

Laboratoire d'Optique Quantique, Ecole Polytechnique, Route de Saclay, 91128 Palaiseau Cedex, France

J.-C. Leicknam and S. Bratos

Laboratoire de Physique Théorique des Liquides, Université Pierre et Marie Curie, Case courrier 121, 4 Place Jussieu, 75252 Paris Cedex 05, France

(Received 22 May 2001; accepted 12 November 2001)

We study the spectral response of the transition between the first and the second excited state of the O–H stretch vibration of HDO dissolved in liquid D₂O with two-color femtosecond mid-infrared spectroscopy. The spectral response of this transition differs strongly from the fundamental absorption spectrum of the O–H stretch vibration. In addition, excitation of the O–H stretch vibration is observed to lead to a change of the hydrogen-bond dynamics of liquid water. We show that both these observations can be described with a refined quantum-mechanical version of the Lippincott–Schroeder model for hydrogen-bonded OH \cdots O systems. © 2002 American Institute of Physics. [DOI: 10.1063/1.1432687]

I. INTRODUCTION

The hydrogen-bond dynamics of liquid water play an important role in chemical processes occurring in aqueous media.^{1,2} For instance, the formation and breaking of hydrogen bonds between water and reacting molecules can strongly affect the kinetics and energetics of chemical reactions. In addition, the hydrogen bonds in liquid water can influence chemical processes by weakening specific chemical bonds. A special but very important example of this effect is the process of proton transfer in liquid water. The formation of an O–H \cdots O hydrogen bond weakens the O–H chemical bond, thereby enabling proton transfer via an exchange of these bonds.^{3,4}

A powerful tool for investigating the dynamics of liquid water is femtosecond mid-infrared spectroscopy. In most of the work using this technique, not pure liquid water, but a dilute solution of HDO in D₂O, an isotopic variety of liquid water, was investigated. The molecular dynamics of this system were observed to be dominated by three time constants: (i) The population relaxation time T_1 of the O–H stretch vibration, for which values between 0.7 and 2 ps have been reported.^{5–12} The value of T_1 exhibits a pronounced temperature⁹ and frequency¹⁰ dependence. (ii) The solvent relaxation time τ_Ω , identical to the O–H frequency-shift correlation time. This time constant was found to be on the order of 1 picosecond,^{5,6,11} in good agreement with the results of molecular dynamics simulations.^{13–17} (iii) The orientational correlation time τ_R , for which a value of approximately 2.5 ps was measured.^{18,19} This value agrees very well with findings from NMR, laser spectroscopic, and molecular dynamics studies.^{20–23} The orientational and hydrogen-bond dynamics of the water molecules are strongly coupled, because the energy barrier for molecular reorientation depends on the length of the hydrogen bond.^{18,19}

In this paper, we report on the investigation of the

excited-state absorption ($\nu_{\text{OH}}=1\rightarrow 2$) of the O–H stretch vibration of HDO dissolved in D₂O with two-color femtosecond mid-infrared spectroscopy. The time-dependence and spectral shape of this excited-state absorption gives new information on the dynamics of hydrogen bonds in liquid water, and on the coupling between the O–H stretch vibration and the O–H \cdots O hydrogen bond.

II. EXPERIMENT

The dynamics of the O–H stretch vibration of HDO dissolved in D₂O are studied with a two-color mid-infrared pump–probe experiment.²⁴ The pulses are generated via parametric amplification processes in BBO and KTP crystals that are pumped by the pulses delivered by a regenerative Ti:sapphire amplifier (100 fs, 800 nm, 1 mJ, 1 kHz). There are two separate chains of parametric amplification processes, in order to produce pump and probe pulses that are independently tunable between 2.7 and 4 μm . The pulse energies are approximately 10 μJ for the pump and 1 μJ for the probe. Both pulses have a duration of approximately 150 fs and are polarized in the same direction. The pump and probe pulses are focused into the sample by separate CaF₂ lenses.

The sample is a solution of 0.5% HDO in D₂O and is contained between two infrasil windows, 200 μm from each other. The absorption spectrum of the O–H stretch vibration of the HDO molecule has its maximum at 3420 cm^{-1} (2.9 μm) and has a width of 260 cm^{-1} . The pump pulse is tuned to a particular frequency in the O–H stretch absorption band, and the spectral response of this excitation is monitored by measuring the probe transmission as a function of probe frequency. More details on the experimental setup can be found in Ref. 24.

Figure 1 presents transient absorption spectra of the O–H stretch vibration at a delay of 300 fs. Each spectrum is obtained with a different central frequency for the pump pulse. For probe frequencies $>3300 \text{ cm}^{-1}$, the signal is posi-

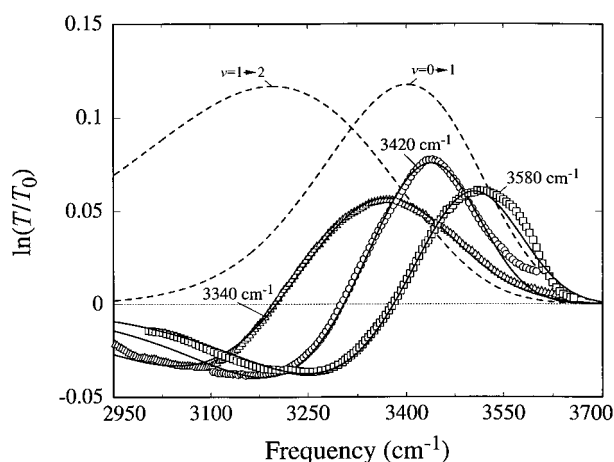


FIG. 1. Transient spectra of an aqueous solution of 0.5% HDO dissolved in D_2O obtained with three different pump pulses. The spectra are measured at a delay of 300 femtoseconds after excitation by the pump pulse. The solid curves represent transient spectra that are calculated with the modified quantum-mechanical Lippincott–Schroeder model described in Sec. III. The dashed curves represent calculated thermal equilibrium $v_{OH}=0 \rightarrow 1$ and $v_{OH}=1 \rightarrow 2$ absorption spectra.

tive and results from the bleaching of the $v_{OH}=0 \rightarrow 1$ transition. For frequencies $<3300 \text{ cm}^{-1}$, the signal is negative and results from the induced $v_{OH}=1 \rightarrow 2$ absorption. For all three pump frequencies, the bleaching is narrower than the $v_{OH}=0 \rightarrow 1$ (linear) absorption band, which means that the excitation leads to the formation of a spectral hole in an inhomogeneously broadened absorption band. Because the O–H stretch frequency is strongly correlated to the O–H \cdots O hydrogen-bond length,^{25,26} the excitation of a spectral hole implies that a subset of the thermal distribution in hydrogen-bond lengths is excited.

Interestingly, the shape of the $v_{OH}=1 \rightarrow 2$ induced absorption spectrum strongly differs from the nearly Gaussian shape of the linear ($v_{OH}=0 \rightarrow 1$) absorption spectrum. The induced absorption is much broader and strongly asymmetric, being much steeper on the high-frequency side than on the low-frequency side. The steep high-frequency side can partly be explained from the cancellation of the bleaching and the induced absorption in this frequency region. However, even after correction for this effect, the induced absorption remains strongly asymmetric.

Figure 2 shows experimental spectra at four different delays after excitation with a pump pulse centered at 3580 cm^{-1} . This excitation is in the blue wing of the absorption spectrum of the O–H stretch vibration. With increasing delay, the spectral hole and the induced absorption show a broadening and a shift to lower frequencies. For the spectral hole this shift has been observed before.^{5,6}

III. QUANTUM-MECHANICAL MODEL FOR THE TRANSIENT SPECTRAL RESPONSE OF LIQUID WATER

A. Spectral response of the O–H stretch vibration in an O–H \cdots O system

The transient spectral response of the $v_{OH}=0 \rightarrow 1$ transition of the O–H stretch vibration of HDO dissolved in

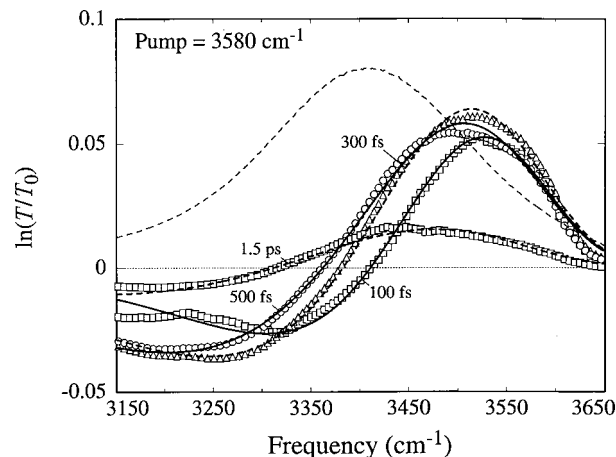


FIG. 2. Transient spectra of an aqueous solution of 0.5% HDO dissolved in D_2O after excitation with a pulse centered at 3580 cm^{-1} . The solid and thick dashed curves represent transient spectra that are calculated with the modified quantum-mechanical Lippincott–Schroeder model described in Sec. III. The thin dashed curve represents the experimental linear absorption spectrum of the O–H stretch vibration.

liquid D_2O has been studied theoretically by several authors, either with a correlation function approach,^{27,28} or with a Brownian oscillator model.^{11,29,30} In this latter model, the effects of hydrogen bonding on the O–H stretch absorption spectrum are described with displaced harmonic hydrogen-bond potentials corresponding to the ground state ($v_{OH}=0$), and the excited state ($v_{OH}=1$). This description yields a Gaussian-shaped linear absorption spectrum, in quite good agreement with the experimentally observed absorption spectrum of the O–H stretch vibration of HDO dissolved in D_2O . From Figs. 1 and 2, it is clear that the $v_{OH}=1 \rightarrow 2$ absorption spectrum has a strongly non-Gaussian shape that cannot be accounted for by the Brownian oscillator model. The description of the $v_{OH}=1 \rightarrow 2$ absorption spectrum requires a more advanced model that, in contrast to the Brownian oscillator model, includes strong anharmonicities for the potentials of the O–H stretch and the O–H \cdots O hydrogen-bond coordinates.

As a starting point for a description of the anharmonic coupling between the O–H stretch vibration and the O–H \cdots O hydrogen-bond mode, we use the so-called Lippincott–Schroeder (LS) model.³¹ This model is based on the experimentally observed strong correlation between the frequency of the O–H stretch vibration and the length of the O–H \cdots O hydrogen bond.^{25,26} This correlation is surprisingly similar for systems that differ in the strength of local electric fields and in the presence of hydrogen-bond interactions other than the O–H \cdots O hydrogen bond. This universal behavior can be explained from the fact that most interactions affect the O–H stretch mode of an O–H \cdots O hydrogen-bonded system mainly by changing the length of the polarizable O–H \cdots O hydrogen bond. These interactions thus have very little effect on the relation between the O–H stretch vibration and the O–H \cdots O hydrogen bond, and mainly express themselves in a change of the length of this bond. Hence, the interactions between the O–H stretch mode of the HDO molecule and its surroundings can be well-described

with a single well-defined relation between the vibrational potential of the O–H stretch mode and the length of the O–H···O. Such a relation is provided by the LS model. Of course, this description is not absolutely perfect, which means that at each O–H···O hydrogen-bond length there will be a narrow distribution of corresponding O–H stretch frequencies.

The potential energy in the LS model is the sum of a potential-energy term V_I that depends both on the length r of the O–H bond and the oxygen–oxygen distance R of the O–H···O hydrogen bond, and a potential-energy term V_{II} that only depends on R . The potential V_I is³¹

$$V_I(r, R) = D_{Ia} [1 - e^{-n_{Ia}(r-r_0)^2/2r}] + D_{Ib} [1 - e^{-n_{Ib}(R-r-r_0)^2/2(R-r)}]. \quad (1)$$

The parameters of $V_I(r, R)$ follow from various experimental observations. The energy D_{Ia} equals the O–H binding energy of water of $38\,750\text{ cm}^{-1}$ (4.8 eV), n_{Ia} is determined by the frequency of the O–H stretch vibration and equals $9.8 \times 10^{10}\text{ m}^{-1}$, r_0 represents the O–H bond length in the gas phase (absence of a hydrogen bond), and has a value of $0.97 \times 10^{-10}\text{ m}$, and D_{Ib} is determined by the relations between the O–H bond length r , the O–H stretch vibrational frequency and the oxygen–oxygen distance R . An excellent description of these relations is obtained with $D_{Ia}/D_{Ib} \approx 1.5$.³¹ Here we use $D_{Ib} = 25\,000\text{ cm}^{-1}$.

In the past, the LS model has mostly been used classically. Only in a recent study by Staib and Hynes,³² the model was used quantum-mechanically to calculate the vibrational lifetime of the O–H stretch vibration. In the original classical treatment, the frequency of the O–H stretch vibration was calculated from the second derivative of the energy in the minimum of the potential-energy curve. Clearly, this procedure gives a rather poor account of the anharmonic character of the potential at energies corresponding to the $\nu_{OH}=1$ and $\nu_{OH}=2$ vibrational states. Therefore, we perform a quantum-mechanical calculation by solving the one-dimensional Schrödinger equation for the O–H coordinate r using the LS potential $V_I(r, R)$. We use an adiabatic approximation with R as a parameter, which implies that the first and second derivative of the vibrational wave functions of the O–H stretch vibration with respect to R are neglected. This type of adiabatic approach is commonly used in describing the coupling between a high-frequency O–H stretch vibration and a low-frequency O–H···O hydrogen bond.^{33–35} The calculation is performed using the numerical Numerov method,³⁶ and results in vibrational eigenfunctions and vibrational energies E_v as a function of R for all states ν_{OH} .

The adiabatic approximation will be valid if the motion in R is much slower than that in r . The characteristic frequencies of the hydrogen-bond vibration of 200 cm^{-1} ,³⁷ and of the O–H stretch vibration of 3400 cm^{-1} indicate that the adiabatic approach is a quite good approximation. Of course, the approximation is not perfect, and there will be a small mixing of the hydrogen-bond levels associated with the $\nu_{OH}=1$ state with high-energy hydrogen-bond levels associated with the $\nu_{OH}=0$ state. As a result, the population that is excited by the pump pulse to the $\nu_{OH}=1$ state, is transferred

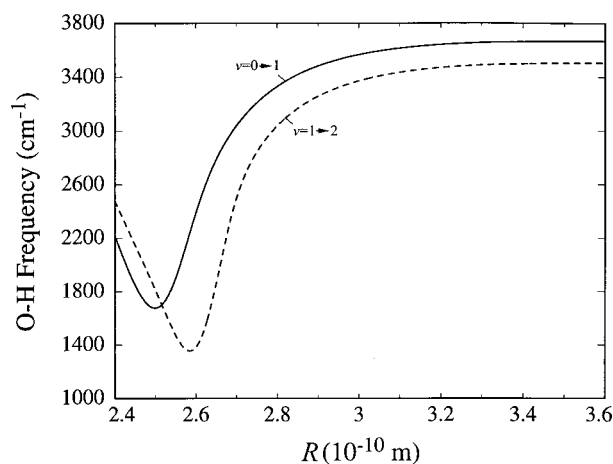


FIG. 3. Calculated frequencies of the $\nu_{OH}=0 \rightarrow 1$ and the $\nu_{OH}=1 \rightarrow 2$ transitions as a function of the oxygen–oxygen distance R of the O–H···O hydrogen bond. These curves are calculated with the modified quantum-mechanical Lippincott–Schroeder model described in the text.

back to the $\nu_{OH}=0$ state with a time constant that is determined by the amount of nonadiabatic mixing. For this population relaxation process, time constants ranging from 0.7–2 picoseconds have been reported.^{5–12}

We can now construct hydrogen-bond potential-energy functions $W_v(R)$ by adding $E_v(R)$ to the potential-energy term $V_{II}(R)$. The hydrogen-bond potentials $W_v(R)$ are used to calculate the transient spectral shapes of the $\nu_{OH}=0 \rightarrow 1$ and $\nu_{OH}=1 \rightarrow 2$ transitions. The comparison of the experimental spectra shown in Figs. 1 and 2 with calculated transient spectra enables an accurate determination of n_{Ib} (the only yet unknown parameter in the potential V_I), and the shape of the additional potential-energy term $V_{II}(R)$. The latter potential represents the electrostatic attraction of two water molecules at large distances and their repulsion at short distances. The experimental transient spectra can be well-fitted using a Morse potential for $V_{II}(R)$:

$$V_{II}(R) = D_{II} [1 - e^{-n_{II}(R-R_0)}]^2. \quad (2)$$

The calculated transient spectra are not very sensitive to the values of D_{II} and R_0 . Therefore these parameters are chosen such that the hydrogen-bond potential $W_0(R) [= E_0(R) + V_{II}(R)]$ of the vibrational ground state of the O–H stretch vibration has the correct average dissociation energy and the correct average equilibrium hydrogen-bond length. We use $D_{II} = 2000\text{ cm}^{-1}$ and $R_0 = 2.88 \times 10^{-10}\text{ m}$. This results in a potential $W_0(R)$ with a dissociation energy of 1900 cm^{-1} and an equilibrium hydrogen-bond length of $2.85 \times 10^{-10}\text{ m}$, in good agreement with the experimental observations.¹ The transient spectra are very sensitive to the values of n_{Ib} and n_{II} . The asymmetry of the $\nu_{OH}=0 \rightarrow 1$ and $\nu_{OH}=1 \rightarrow 2$ absorption bands is strongly determined by n_{Ib} , and the width of these bands depends on n_{II} . From a simultaneous fit of n_{Ib} and n_{II} to the transient spectra, we find $n_{Ib} = 16.5(1.0) \times 10^{10}\text{ m}^{-1}$ and $n_{II} = 2.9(0.2) \times 10^{10}\text{ m}^{-1}$. The value of n_{Ib} implies that $D_{Ia}n_{Ia} \approx D_{Ib}n_{Ib}$, as was the case in the original classical version of the LS model.³¹

Figure 3 shows the frequencies of the $\nu_{OH}=0 \rightarrow 1$ and $\nu_{OH}=1 \rightarrow 2$ transitions as a function of the oxygen–oxygen

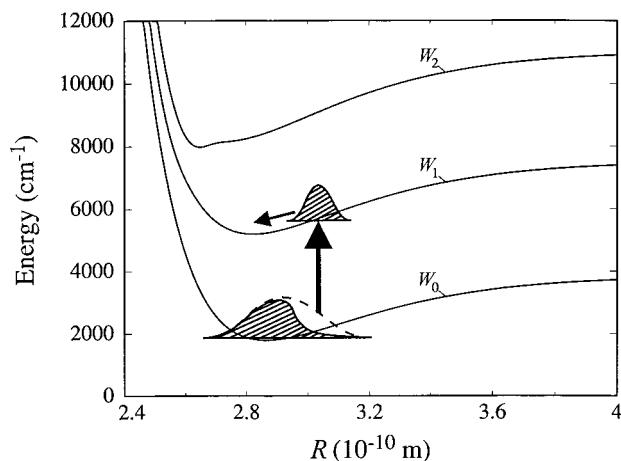


FIG. 4. Hydrogen-bond potentials for the $\nu_{\text{OH}}=0, 1, 2$ states. These functions are obtained by fitting the parameters of the modified quantum-mechanical Lippincott–Schroeder model to the transient spectra of Figs. 1 and 2. Also shown is a schematic picture of the burning of a spectral hole in the thermal hydrogen-bond distribution in W_0 and the generation of a non-equilibrium distribution in W_1 .

distance R . The calculated $\nu_{\text{OH}}=0 \rightarrow 1$ transition frequency shows a strongly nonlinear dependence on R , in good agreement with experimental observations.^{25,26} Figure 4 shows the hydrogen-bond potentials $W_0(R)$, $W_1(R)$ and $W_2(R)$ (corresponding to $\nu_{\text{OH}}=0, 1, 2$ states).

The origin of the large width and asymmetric shape of the $\nu_{\text{OH}}=1 \rightarrow 2$ absorption spectrum can be understood from the change of the distribution in R upon excitation of the O–H stretch vibration. We find that the hydrogen bond shortens from $R_{\text{eq},0}=2.85 \times 10^{-10}$ m in $\nu_{\text{OH}}=0$ to $R_{\text{eq},1}=2.80 \times 10^{-10}$ m in $\nu_{\text{OH}}=1$ and $R_{\text{eq},2}=2.65 \times 10^{-10}$ m in $\nu_{\text{OH}}=2$. Figure 3 shows that the $\nu_{\text{OH}}=0 \rightarrow 1$ and $\nu_{\text{OH}}=1 \rightarrow 2$ transition frequencies change more rapidly with R at small values of R than at large values of R . Hence, for a given distribution of R , the spectral response of the transition between two neighboring states of the O–H vibration will broaden with increasing vibrational quantum number. The $\nu_{\text{OH}}=1 \rightarrow 2$ transition frequency changes very rapidly in the interval 2.6×10^{-10} m $< R < 2.9 \times 10^{-10}$ m that corresponds to the thermal distribution of R in the $\nu_{\text{OH}}=1$ state. The rapid change of the $\nu_{\text{OH}}=1 \rightarrow 2$ transition frequency in this interval can be explained from the shape of the r -dependent potential-energy contribution $V_1(r, R)$. In Fig. 5, the potential $V_1(r, R)$ is shown as a function of the O–H bond length for three values of the oxygen–oxygen distance R . At oxygen–oxygen distances R below 2.7×10^{-10} m, the potential $V_1(r, R)$ becomes very broad at energies that correspond to the energy of the $\nu_{\text{OH}}=2$ state. This broadening of the potential leads to a strong decrease of E_2 . Hence, in this region of R , a small variation in R leads to a large change of E_2 . As a result, the transition frequency of the $\nu_{\text{OH}}=1 \rightarrow 2$ transition varies strongly over the thermal distribution of R (with a width of $\approx 3.6 \times 10^{-11}$ m at 300 K), which leads to a strong broadening of the $\nu_{\text{OH}}=1 \rightarrow 2$ transition.

B. Calculation of transient spectra

To calculate the transient spectra, the potentials $W_\nu(R)$ are calculated in 400 points between $R=2.2 \times 10^{-10}$ m and

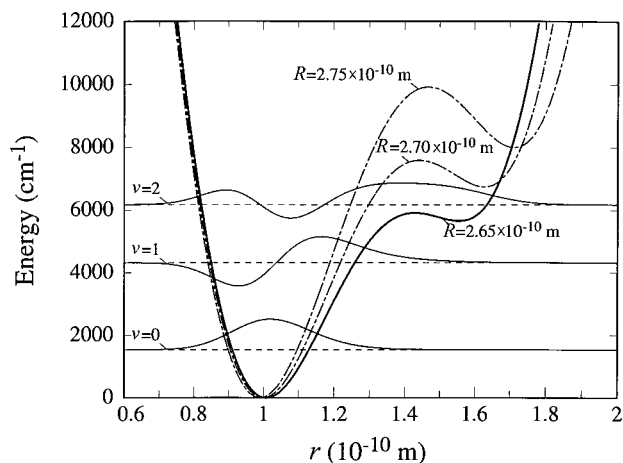


FIG. 5. Vibrational potential V_1 for three different oxygen–oxygen distances R of the O–H···O hydrogen bond as a function of the O–H bond length r . Also shown are the vibrational wave functions of the $\nu_{\text{OH}}=0, 1, 2$ states for $R=2.65 \times 10^{-10}$ m.

$R=3.8 \times 10^{-10}$ m. In the same 400 points, the transition dipole matrix element between the wave functions belonging to $\nu_{\text{OH}}=0, 1, 2$ are calculated: $\mu_{01}(R)=\langle \phi_1(r;R)|r|\phi_0 \times(r;R) \rangle$, $\mu_{12}(R)=\langle \phi_2(r;R)|r|\phi_1(r;R) \rangle$. The excitation-induced hole $\Delta n_0(R)$ in the thermal population distribution of $W_0(R)$, and the excited population distribution $\Delta n_1(r)$ in $W_1(R)$ are proportional to the spectral intensity of the pump and the linear absorption cross section, both at the frequency $\nu(R)=[W_1(R)-W_0(R)]/h$, with h Planck's constant. In calculating $\Delta n_0(R)$ and $\Delta n_1(R)$, we also consider the homogeneous contribution to the absorption linewidth. The homogeneous broadening smoothens the correlation between R and the transition frequency $\nu(R)$, and thus broadens $\Delta n_0(R)$ and $\Delta n_1(R)$. To account for the effects of homogeneous broadening in the excitation process, the pump–pulse spectrum is convoluted with a Lorentzian with a width of 90 cm^{-1} before calculating $\Delta n_0(R)$ and $\Delta n_1(R)$. This homogeneous width of 90 cm^{-1} is in good agreement with the result of a recent femtosecond mid-infrared photon-echo study of HDO dissolved in D_2O .³⁸

The distributions $\Delta n_0(R)$ and $\Delta n_1(R)$ are delay-dependent, because the pump is a Gaussian pulse with a pulse duration of approximately 150 femtoseconds, and because R changes in time (these dynamics are described in the following subsection). The transient spectrum at a particular delay after the pump is calculated by multiplying $\Delta n_0(R)$ and $\Delta n_1(R)$ with the R -dependent transition probabilities of the $\nu_{\text{OH}}=0 \rightarrow 1$, $\nu_{\text{OH}}=1 \rightarrow 0$, and $\nu_{\text{OH}}=1 \rightarrow 2$ transitions, to determine the bleaching contribution, the stimulated emission contribution and the excited-state absorption contribution to the transient spectrum, respectively. To obtain the final calculated transient spectrum, the three contributions are added and convoluted with the probe spectrum and a Lorentzian with a full width at half maximum of 90 cm^{-1} , that represents the homogeneous contribution to the absorption spectrum.

C. Hydrogen-bond dynamics in different O–H stretch vibrational states

In principle, the hydrogen-bond dynamics within each of the adiabatic hydrogen-bond potentials $W_v(R)$ could be calculated by solving the one-dimensional Schrödinger equation in R with $W_v(R)$ as the potential. This type of description would be appropriate for gas-phase hydrogen-bonded clusters in which the hydrogen-bond vibration is underdamped. For these systems, the coupling between the O–H stretch vibration and the hydrogen-bond mode leads to a hydrogen-bond vibrational (Franck–Condon) progression of the absorption spectrum of the O–H stretch vibration.³⁹ However, in the liquid phase, the linear and transient absorption spectra of HDO:D₂O do not contain sidebands and are very broad. This indicates that the hydrogen-bond vibrations of liquid water are strongly overdamped, which implies that the wave functions in R are strongly coupled to each other and to other low-frequency liquid modes. The dynamics in R are therefore not determined by the level spacing of the unperturbed vibrational levels of the hydrogen-bond mode, but rather result from a stochastic modulation of the value of R due to the frictional interactions with the surrounding liquid. This type of dynamics can best be described as a diffusion process in the potential $W_v(R)$.

If the hydrogen-bond potentials were harmonic, the diffusive hydrogen-bond dynamics could be described analytically.^{11,29,30} However, for the strongly anharmonic potentials W_0 , W_1 , and W_2 that result from the LS model, the hydrogen-bond dynamics must be calculated numerically. We describe the hydrogen-bond dynamics with classical wave packets of which the dynamics are allowed to be different on the $W_0(R)$ and $W_1(R)$ hydrogen-bond potentials. In related previous microscopic semiclassical treatments, the dynamics on the potential-energy surfaces of the ground and excited state were calculated using molecular dynamics simulations.^{40–42} Here, we describe the dynamics of the hydrogen bonds as a diffusion process in a potential well $W_v(R)$. As a result of this diffusion, the excited distribution $\Delta n_v(R, t)$ of hydrogen bond lengths equilibrates to a thermal distribution in the potential $W_v(R)$.

The time dependence of $\Delta n_0(R, t)$ and $\Delta n_1(R, t)$ that results from the stochastic modulation of the oxygen–oxygen distance, is calculated with a diffusion equation:⁴³

$$\frac{\partial \Delta n_v}{\partial t} = \frac{L_v^2}{2\tau_D} \left(\frac{\partial^2 \Delta n_v}{\partial R^2} + \beta \Delta n_v \frac{\partial^2 W_v}{\partial R^2} + \beta \frac{\partial \Delta n_v}{\partial R} \frac{\partial W_v}{\partial R} \right), \quad (3)$$

where β is the Boltzmann factor $1/k_B T$, L_v is the half-width at $1/e$ of the maximum of the equilibrium distribution in the potential $W_v(R)$, and τ_D is the characteristic time scale for the diffusion process. For τ_D we used a value of 700 femtoseconds, equal to the measured autocorrelation time constant of R .⁵ We solve Eq. (3) numerically by discretizing the R and t in steps $\delta R = 0.4 \times 10^{-12}$ m and $\delta t = 2$ fs, respectively. The time constant τ_s for the transfer of population between two bins is related to τ_D via $\tau_s = 2\tau_D(\delta R/L_v)^2$ in the case of a hop downhill in potential energy ($\delta W_v < 0$). For a hop uphill ($\delta W_v > 0$), $\tau_s = 2\tau_D(\delta R/L_v)^2 \exp(\beta \delta W_v)$.

For a system with harmonic potentials and Gaussian-shaped spectra, the spectral diffusion can be described with the following autocorrelation function for the detuning $\delta\omega(t)$ of an oscillator from the center of the absorption band^{11,29}

$$\langle \delta\omega(t) \delta\omega(0) \rangle = D^2 e^{-t/\tau_\Omega}, \quad (4)$$

where D is the half-width at $1/e$ of the maximum of the Gaussian spectrum. The value of τ_Ω can be determined from the time dependence of the first moment of the transient spectrum.⁵ For harmonic potentials τ_Ω is exactly the same as τ_D that enters Eq. (3).⁴⁴ For the nonparabolic hydrogen-bond potentials W_v that follow from the LS model, this is no longer true. However, we find that for the hydrogen-bond potentials W_v the value of τ_Ω , as it can be determined from the delay dependence of the calculated first spectral moment, negligibly differs from the hydrogen-bond diffusion time constant τ_D . Therefore, in the following we will use $\tau_D = \tau_\Omega$.

The model given above describes the hydrogen-bond dynamics in each of the individual potentials $W_v(R)$, which means that this description presumes the validity of the adiabatic approximation. It should be noted that for oscillators that show a nonadiabatic transition from $W_1(R)$ to $W_0(R)$, the hydrogen-bond dynamics will likely be different, since a nonadiabatic transition leads to a strong increase of the kinetic energy of the hydrogen-bond motion. However, a nonadiabatic transition also implies that the O–H oscillator has returned to the vibrational ground state, which implies that the oscillator is no longer observed in the $\nu_{\text{OH}}=0 \rightarrow 1$ bleaching signal and the $\nu_{\text{OH}}=1 \rightarrow 2$ induced absorption. This means that the hydrogen-bond dynamics observed in the transient spectra form the adiabatic dynamics, i.e., the dynamics of those oscillators that do not undergo nonadiabatic transitions.

IV. DISCUSSION

The modeling of the hydrogen-bond dynamics with a single diffusive process does not provide a good description of the transient spectra of Figs. 1 and 2, especially in the region of the $\nu_{\text{OH}}=1 \rightarrow 2$ transition. This is illustrated in Fig. 6, in which the frequency at which the induced absorption changes into a bleaching is presented as a function of delay for a pump frequency of 3580 cm^{-1} (corresponding to the data of Fig. 2). The experimentally observed frequencies are compared with the results of two calculations in which the hydrogen-bond dynamics is purely diffusive. At short delay times (< 500 fs), the experimentally observed zero-crossings can be well-fitted with a fast diffusion process with a time constant $\tau_\Omega = 600$ fs, but for longer delay times (> 1 ps), this gives a poor description of the experimental observations. At these longer delay times, a much better description is obtained with a slow diffusion process with a time constant $\tau_\Omega = 950$ fs. Hence, we observe that in the first 500 fs after excitation, the transient spectra show a rapid shift to lower frequencies. This rapid shift is followed by a much slower evolution to the final thermal distribution.

During the first 500 femtoseconds, the transient spectrum changes more rapidly at frequencies $< 3450 \text{ cm}^{-1}$ than

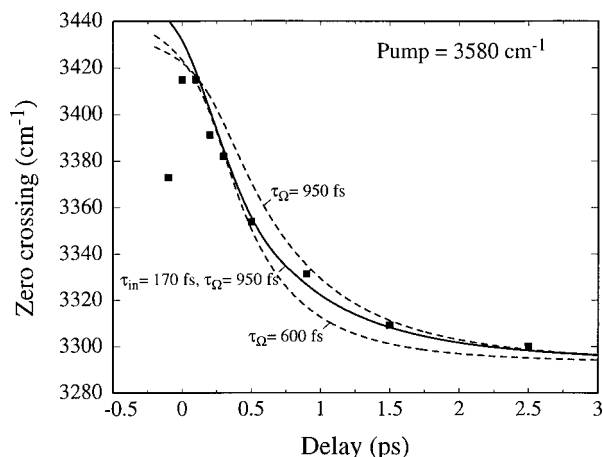


FIG. 6. Frequency at which the bleaching in the transient spectrum changes into an induced absorption as a function of delay. The points are obtained by exciting the O–H stretch vibration of a solution of 0.5% HDO in D₂O at 3580 cm⁻¹. The dashed curves represent calculations in which the hydrogen-bond length is stochastically modulated (diffusion) in the hydrogen-bond potentials W_0 and W_1 . The solid curve represents a calculation in which the hydrogen bond is stochastically modulated and in addition experiences a fast shift with a time constant $\tau_{in}=170\pm 40$ fs towards the minimum of the W_1 potential.

at frequencies >3550 cm⁻¹, which indicates that the fast process has a much stronger effect on the $\nu_{OH}=1\rightarrow 2$ induced absorption spectrum than on the $\nu_{OH}=0\rightarrow 1$ bleaching signal. This observation shows that the fast component is only active in the $\nu_{OH}=1$ state. The solid curves in Figs. 1, 2, and 6 represent the results of a calculation in which the hydrogen-bond length is stochastically modulated in the $\nu_{OH}=0$ and $\nu_{OH}=1$ state with a time constant of 950 ± 100 fs, and in which the excited distribution $n(R,t)$ on the $\nu_{OH}=1$ potential has an additional rapid shift over a limited distance, directly following its excitation. This shift, which depends on the elapsed time since excitation, cannot easily be incorporated in the time-invariant diffusion equation Eq. (3). Therefore, we model the initial shift phenomenologically in the numerical calculation, with time steps δt and excitation time t_{ex} , with the transformation

$$\Delta n_1(R, t + \delta t) = \Delta n_1(R + \Lambda \delta t, t), \quad (5)$$

$$\Lambda = (S/\tau_{in}) \exp((t_{ex} - t)/\tau_{in}). \quad (6)$$

In the description of this shift we incorporated the nonzero pulse duration of the pump and probe pulses. From a fit to the transient spectra of Fig. 2 that were obtained with a pump-pulse of 3580 cm⁻¹, we find $S = (5.6 \pm 1.2) \times 10^{-12}$ m for the total distance over which this shift occurs, and $\tau_{in} = 170 \pm 40$ fs. This value of S corresponds to $45 \pm 10\%$ of the distance between the center of the initially excited hydrogen-bond length distribution and the minimum of the $W_1(R)$ potential.

The presence of a fast initial component in the hydrogen-bond dynamics of the $\nu_{OH}=1$ state can be explained as follows. The oscillation in the hydrogen-bond coordinate is overdamped, which means that each individual oscillator will have a local hydrogen-bond potential that is determined both by the potential W_0 and by the local configuration of the liquid. The excitation with a short pump-

pulse to the $\nu_{OH}=1$ state leads to a rapid change of W_0 to W_1 , and thereby to a change of the local potential. This change of the local potential induces a rapid adaptation of the hydrogen-bond length. For the hole that is burnt in $\nu_{OH}=0$, the local potential does not change, and therefore the dynamics of the hole only result from the diffusive reorganization of the local liquid structure. The presence of a significant fast component in the hydrogen-bond dynamics of liquid water implies that water molecules can adapt to changes in charge distribution or molecular orientation (for instance as a result of chemical reactions) on a time scale that is much shorter than that of the spontaneous reorganization of the liquid.

The time constant $\tau_{in} = 170 \pm 40$ fs of the contraction of the hydrogen-bond length in the $\nu_{OH}=1$ state is much shorter than the time constant $\tau_{\Omega} = 950 \pm 100$ fs of the spontaneous reorganization of the liquid. This suggests that the fast initial response is a local effect, involving only a few water molecules. Nevertheless, τ_{in} is still much longer than a quarter of the oscillation period of approximately 160 fs (200 cm⁻¹) of the undamped O–H··O hydrogen-bond stretch vibration. Hence, the fast adaptation of the hydrogen-bond length is still an overdamped motion. The time constant $\tau_{in} = 170 \pm 40$ fs is very similar to that of the fast component of the dielectric relaxation of liquid water that was recently observed with THz reflection spectroscopy.^{45,46} This fast dielectric component was also assigned to a local reorganization involving only one or a few water molecules.

V. CONCLUSIONS

In conclusion, we investigated the spectral response of the excited-state absorption ($\nu_{OH}=1\rightarrow 2$) of HDO dissolved in D₂O on a femtosecond time scale. We found that this response is strongly asymmetric and much broader than the linear ($\nu_{OH}=0\rightarrow 1$) absorption spectrum. The spectral shape of the $\nu_{OH}=1\rightarrow 2$ transition can be explained from the strong anharmonic interactions between the O–H stretch vibration and the O–H··O hydrogen-bond. These anharmonic interactions are quantitatively described with a refined quantum-mechanical version of the Lippincott–Schroeder model. This model also provides an accurate description of the relations between the hydrogen-bond length, the O–H bond length and the O–H stretch frequency.

From a detailed study of the transient spectral responses at different delays, we find that the dynamics of the hydrogen-bond length in both the $\nu_{OH}=0$ and the $\nu_{OH}=1$ state of the O–H stretch vibration are diffusive process with a time constant $\tau_{\Omega} = 950 \pm 100$ fs. These diffusive dynamics result from the spontaneous reorganizations of liquid water. For the $\nu_{OH}=1$ state, the hydrogen-bond dynamics contain an additional fast component with a time constant $\tau_{in} = 170 \pm 40$ fs. This fast component is observed directly after excitation of the $\nu_{OH}=1$ state out of $\nu_{OH}=0$, and results from the rapid contraction of the hydrogen bond towards its new equilibrium position in this state.

ACKNOWLEDGMENTS

The research presented in this paper is part of the research program of the Stichting Fundamenteel Onderzoek der Materie (Foundation for Fundamental Research on Matter) and was made possible by financial support from the Nederlandse Organisatie voor Wetenschappelijk Onderzoek (Netherlands Organization for the Advancement of Research) (H.J.B. and H.-K.N.). The authors wish to thank the Center National de la Recherche Scientifique for financial support (G.G., N.L., G.M.G., J.-C.L., and S.B.).

- ¹D. Eisenberg and W. Kautzmann, *The Structure and Properties of Water* (Oxford University Press, New York, 1969).
- ²P. Schuster, G. Zundel, and C. Sandorfy, *The Hydrogen Bond* (North Holland, Amsterdam, 1976).
- ³C. J. T. de Grotthuss, *Ann. Chim. (Paris)* **LVIII**, 54 (1806).
- ⁴D. Marx, M. E. Tuckerman, J. Hutter, and M. Parrinello, *Nature (London)* **397**, 601 (1999).
- ⁵G. M. Gale, G. Gallot, F. Hache, N. Lascoux, S. Bratos, and J.-C. Leicknam, *Phys. Rev. Lett.* **82**, 1068 (1999).
- ⁶S. Bratos, G. M. Gale, G. Gallot, F. Hache, N. Lascoux, and J.-C. Leicknam, *Phys. Rev. E* **61**, 5211 (2000).
- ⁷R. Laenen, C. Rauscher, and A. Laubereau, *Phys. Rev. Lett.* **80**, 2622 (1998).
- ⁸R. Laenen, C. Rauscher, and A. Laubereau, *J. Phys. Chem. B* **102**, 9304 (1998).
- ⁹S. Woutersen, U. Emmerichs, H.-K. Nienhuys, and H. J. Bakker, *Phys. Rev. Lett.* **81**, 1106 (1998).
- ¹⁰G. M. Gale, G. Gallot, and N. Lascoux, *Chem. Phys. Lett.* **311**, 113 (1999).
- ¹¹S. Woutersen and H. J. Bakker, *Phys. Rev. Lett.* **83**, 2077 (1999).
- ¹²J. C. Deak, S. T. Rhea, L. K. Iwaki, and D. D. Dlott, *J. Phys. Chem. A* **104**, 4866 (2000).
- ¹³F. Sciortino, P. H. Poole, H. E. Stanley, and S. Havlin, *Phys. Rev. Lett.* **64**, 1686 (1990).
- ¹⁴A. Luzar and D. Chandler, *Phys. Rev. Lett.* **76**, 928 (1996).
- ¹⁵J. Marti, J. Padro, and E. Guardia, *J. Chem. Phys.* **105**, 639 (1996).
- ¹⁶M. Diraison, Y. Guissani, J.-C. Leicknam, and S. Bratos, *Chem. Phys. Lett.* **258**, 348 (1996).
- ¹⁷A. Chandra, *Phys. Rev. Lett.* **85**, 768 (2000).
- ¹⁸H. J. Bakker, S. Woutersen, and H.-K. Nienhuys, *Chem. Phys.* **258**, 233 (2000).
- ¹⁹H.-K. Nienhuys, R. A. van Santen, and H. J. Bakker, *J. Chem. Phys.* **112**, 8487 (2000).
- ²⁰D. W. G. Smith and J. G. Powles, *Mol. Phys.* **10**, 451 (1966).
- ²¹M. Nakahara, in *Physical Chemistry of Aqueous Systems*, edited by H. J. White, Jr., J. V. Sengers, B. D. Neumann, and J. C. Bellows (Begell House, New York, 1995), p. 449.
- ²²D. V. Belle, M. Froyen, G. Lippens, and S. Wodak, *Mol. Phys.* **72**, 239 (1992).
- ²³I. Svishchev and P. Kusalik, *J. Phys. Chem.* **98**, 728 (1994).
- ²⁴G. Gallot, Ph.D. thesis, Ecole Polytechnique, Palaiseau, France (1998).
- ²⁵A. Novak, *Struct. Bonding (Berlin)* **18**, 177 (1974).
- ²⁶W. Mikenda, *J. Mol. Struct.* **147**, 1 (1986).
- ²⁷S. Bratos and J.-Cl. Leicknam, *J. Chem. Phys.* **101**, 4536 (1994).
- ²⁸S. Bratos and J.-Cl. Leicknam, *J. Chem. Phys.* **103**, 4887 (1995).
- ²⁹A. I. Burshtein, B. M. Chernobrod, and A. Y. Sivachenko, *J. Chem. Phys.* **110**, 1931 (1999).
- ³⁰S. Mukamel, *Principles of Nonlinear Optical Spectroscopy* (Oxford University Press, New York, 1995).
- ³¹E. R. Lippincott and R. Schroeder, *J. Chem. Phys.* **23**, 1099 (1955).
- ³²A. Staib and J. T. Hynes, *Chem. Phys. Lett.* **204**, 197 (1993).
- ³³Y. Marechal and A. Witkowski, *J. Chem. Phys.* **48**, 3697 (1968); A. Witkowski, *J. Chem. Phys.* **52**, 4403 (1970).
- ³⁴S. Bratos, *J. Chem. Phys.* **63**, 3499 (1975).
- ³⁵B. Boulil and O. Henri-Rousseau, *Chem. Phys.* **126**, 263 (1988).
- ³⁶G. Dahlquist, A. Björck, and N. Anderson, *Numerical Methods* (Prentice-Hall, Englewood Cliffs, NJ, 1974).
- ³⁷L. Thrane, R. H. Jacobsen, P. U. Jepsen, and S. R. Keiding, *Chem. Phys. Lett.* **240**, 330 (1995).
- ³⁸J. Stenger, D. Madsen, P. Hamm, E. T. J. Nibbering, and T. Elsaesser, *Phys. Rev. Lett.* **87**, 027401 (2001).
- ³⁹G. N. Robertson and J. Yarwood, *Chem. Phys.* **32**, 267 (1978).
- ⁴⁰M. Maroncelli and G. R. Fleming, *J. Chem. Phys.* **89**, 5044 (1988).
- ⁴¹E. A. Carter and J. T. Hynes, *J. Chem. Phys.* **54**, 5961 (1991).
- ⁴²L. E. Fried, N. Bernstein, and S. Mukamel, *Phys. Rev. Lett.* **68**, 1842 (1992).
- ⁴³R. Kubo, M. Toda, and N. Hashitsume, *Statistical Physics II, Nonequilibrium Statistical Mechanics* (Springer, Berlin, 1995).
- ⁴⁴A. I. Burshtein and V. S. Malinovsky, *J. Opt. Soc. Am. B* **8**, 1098 (1991).
- ⁴⁵C. Rønne, L. Thrane, P.-O. Åstrand, A. Wallqvist, K. V. Mikkelsen, and S. Keiding, *J. Chem. Phys.* **107**, 5319 (1997).
- ⁴⁶C. Rønne, P.-O. Åstrand, and S. Keiding, *Phys. Rev. Lett.* **82**, 2888 (1999).